Journal of Ovonic Research Vol. 20, No. 6, November - December 2024, p. 813 - 829

Synthesis and characterization of Nano-ZnO incorporated polyurethane-chitosan composite films

B. Zhang, Lei Yu *
Health College, Chongqing Industry & Trade Polytechnic, Fuling 408000, Chongqing, China

This study developed novel polyurethane-chitosan/zinc oxide (PU/CS/ZnO) nanocomposite films for food packaging applications. ZnO nanoparticles were synthesized via a green approach using Mentha pulegium leaf extract and incorporated into PU/CS blends at various concentrations. The PU/CS/ZnO-5% nanocomposite exhibited optimal performance across multiple properties. XRD and FTIR analyses confirmed the successful incorporation of ZnO nanoparticles (average crystallite size 28 nm) and their interaction with the polymer matrix. SEM and TEM imaging revealed uniform dispersion of ZnO nanoparticles throughout the film. The results of mechanical testing indicated a significant improvement in both tensile strength and Young's modulus, with a 51% increase in the former and a 68% increase in the latter when compared to the pure PU/CS blend. UV-vis spectroscopy demonstrated excellent UV-blocking ability, with a UV protection factor of 42.7 for the PU/CS/ZnO-5% film. The nanocomposite films exhibited enhanced antioxidant activity, with a 110% increase in DPPH radical scavenging activity for the PU/CS/ZnO-5% sample. Biodegradability studies showed 58.1% weight loss after 12 weeks of soil burial. Shelf-life extension studies on strawberries revealed that the PU/CS/ZnO-5% film significantly outperformed commercial LDPE packaging, with only 4.2% weight loss and 78.5% firmness retention after 14 days of storage. The nanocomposite films also demonstrated antimicrobial properties, with reduced microbial growth on packaged strawberries. These results highlight the potential of PU/CS/ZnO nanocomposite films as multifunctional, biodegradable packaging materials for perishable foods.

(Received September 4, 2024; Accepted November 18, 2024)

Keywords: Nanocomposite, Barrier properties, Antioxidant activity, Shelf-life extension, Biodegradable packaging

1. Introduction

In recent times, there has been a notable increase in interest towards the creation of innovative materials for packaging purposes. This is largely attributed to the rising environmental issues and the demand for improved methods of food preservation [1]. Polymer nanocomposites

* Corresponding authors: Leiyu_scut@163.com
https://doi.org/10.15251/JOR.2024.206.813

have shown great potential due to their distinct properties arising from the combination of the polymer matrix and nanoscale fillers, making them a promising choice among the materials studied [2,3]. In this context, the integration of biodegradable polymers with inorganic nanoparticles offers an exciting avenue for creating multifunctional packaging materials that address the limitations of conventional plastics while providing additional benefits [4]. Polyurethane (PU) and chitosan (CS) are two versatile biomaterials that have been extensively studied for diverse applications, including packaging [5]. PU, a class of polymers containing urethane linkages, is known for its excellent mechanical properties, flexibility, and durability [6]. These characteristics make PU an attractive choice for packaging materials that require good strength and elasticity [7]. CS, a natural polysaccharide extracted from chitin, has attracted interest for its ability to degrade naturally, compatibility with living organisms, and natural antimicrobial qualities [8]. The combination of PU and CS in a blend or composite system can potentially synergize their individual strengths, resulting in materials with enhanced performance for packaging applications [9].

The integration of nanoparticles into polymer matrices has transformed the materials science industry, leading to the development of nanocomposites that exhibit enhanced properties in comparison to conventional bulk materials [10–12]. Zinc oxide (ZnO) nanoparticles have garnered significant attention for their distinct physical and chemical characteristics compared to other nanofillers [13]. ZnO nanoparticles exhibit antimicrobial activity, UV-blocking capabilities, and photocatalytic properties, making them particularly suitable for packaging applications. When integrated into polymer matrices, ZnO nanoparticles can impart these beneficial characteristics to the resulting nanocomposite, potentially enhancing its functionality and performance [14–16]. The development of PU/CS/ZnO nanocomposite films represents a promising approach to creating advanced packaging materials with multifunctional properties. By combining the structural integrity of PU, the biodegradability of CS, and the functional attributes of ZnO nanoparticles, it is possible to engineer films that address multiple requirements simultaneously [17]. The nanocomposite films show promise in enhancing mechanical strength, increasing resistance to moisture and gases, and providing UV protection. These properties are essential for prolonging the shelf life of packaged goods and maintaining food safety.

The synthesis of PU/CS/ZnO nanocomposite films involves careful consideration of various parameters to achieve optimal performance. The method of ZnO nanoparticle synthesis plays a crucial role in determining their size, morphology, and surface properties, which in turn influence their interaction with the polymer matrix and overall composite properties [18]. Green synthesis methods utilizing plant extracts have gained attention as environmentally friendly alternatives to conventional chemical synthesis, offering the potential for producing ZnO nanoparticles with unique characteristics [19]. The blending of PU and CS presents challenges due to their inherent differences in chemical structure and properties. Achieving a homogeneous blend requires careful optimization of processing conditions and potentially the use of compatibilizers to enhance interfacial interactions. The incorporation of ZnO nanoparticles into the PU/CS blend introduces additional complexity, as the dispersion and distribution of nanoparticles within the polymer matrix significantly impact the final properties of the nanocomposite films.

Characterization of PU/CS/ZnO nanocomposite films is essential to understand their structure-property relationships and evaluate their potential for packaging applications. A comprehensive characterization approach involves the use of various analytical techniques to probe different aspects of the nanocomposite system. XRD and FTIR spectroscopy provide insights into

the crystalline structure and chemical interactions within the nanocomposite. Electron microscopy techniques such as SEM allow visualization of the nanoparticle dispersion and morphology of the films. Mechanical testing is crucial to assess the strength, flexibility, and overall structural integrity of the nanocomposite films. Barrier property measurements, including water vapor transmission rate and oxygen permeability, are vital for evaluating the films' effectiveness in preserving packaged contents. UV-visible spectroscopy can reveal the optical properties and UV-blocking capability of the nanocomposite films. Antioxidant activity tests can assess their potential in preventing oxidation of packaged foods. Biodegradability studies are necessary to confirm the environmental sustainability of the nanocomposite films. The development of PU/CS/ZnO nanocomposite films holds great promise for advancing the field of packaging materials. By combining the strengths of each component – the mechanical robustness of PU, the biodegradability of CS, and the multifunctional properties of ZnO nanoparticles – these nanocomposites have the potential to address multiple challenges in food packaging simultaneously. The ability to tailor the properties of these films through careful control of composition and processing parameters offers opportunities for creating customized packaging solutions for various applications.

This study aims to synthesize and characterize novel PU/CS/ZnO nanocomposite films for potential use in packaging applications. The research seeks to explore the green synthesis of ZnO nanoparticles, optimize the composition of PU-CS blends, and fabricate nanocomposite films with varying ZnO concentrations. Through extensive characterization of structural, morphological, mechanical, barrier, optical, and biodegradation properties, this work aims to evaluate the potential of these nanocomposite films for food packaging applications. Additionally, shelf-life extension studies will be conducted to assess the practical efficacy of the developed materials in preserving food quality.

2. Materials and methods

2.1. Synthesis of ZnO nanoparticles

The synthesis of ZnO nanoparticles was carried out through a sustainable method utilizing Mentha pulegium leaf extract to reduce and stabilize the particles. Fresh Mentha pulegium leaves (50 g) were thoroughly washed with ultrapure water and finely chopped. The leaves were boiled in 500 mL of purified water at 80°C for half an hour with continuous stirring. After that, the extract was filtered using filter paper and kept in a refrigerator at 4°C for future use.

To create ZnO nanoparticles, a solution of zinc acetate dihydrate was prepared by mixing 50 mL of the compound with ultrapure water. Under continuous stirring, 25 mL of the Mentha pulegium leaf extract was added dropwise to the zinc acetate solution. The mixture's pH was raised to 12 by adding a 2 M NaOH solution. The reaction was then left to occur at 60°C for 2 hours with continuous stirring. After centrifuging at 8000 rpm for 15 minutes, the pale white precipitate was collected, washed multiple times with ultrapure water and ethanol to eliminate impurities, and then dried in a hot air oven at 80°C for 12 hours. Subsequently, the dried powder underwent calcination at 400°C for 2 hours in a muffle furnace to produce crystalline ZnO nanoparticles.

2.2. Preparation of PU-CS Blend

The PU-CS blend was prepared using a solution casting method. A 2% w/v CS solution was created by mixing CS powder with a 1% (v/v) acetic acid solution and stirring for a full day at room temperature. PU solution (5% w/v) was prepared by dissolving PU pellets in N,N-dimethylformamide (DMF) at 60°C for 6 hours under constant stirring. The two solutions were then mixed in various ratios (PU:CS = 70:30, 60:40, 50:50 w/w) to optimize the blend composition. The mixtures were homogenized using a high-speed homogenizer (Shanghai Bilon Instrument Co., Ltd.) at 10,000 rpm for 15 minutes to ensure uniform dispersion.

2.3. Fabrication of PU/CS/ZnO nanocomposite films

The fabrication of PU/CS/ZnO nanocomposite films involved a solution casting method. The optimized PU/CS blend (60:40 w/w) was used as the base matrix. ZnO nanoparticles were incorporated into the blend at different concentrations (1, 3, 5, and 7 wt% with respect to the total polymer weight). The required amount of ZnO nanoparticles was first dispersed in a small volume of DMF using ultrasonication for 30 minutes to ensure uniform dispersion. This ZnO dispersion was then added to the PU/CS blend solution and homogenized at 12,000 rpm for 20 minutes to achieve a uniform distribution of nanoparticles within the polymer matrix.

The homogenized solutions were cast onto clean glass plates (20 cm × 20 cm) and dried. The dried films were subsequently removed and placed in a vacuum oven at 40°C for 24 hours to eliminate remaining solvent. Films with an average thickness of 100 ± 5 μm were used for further characterization and testing.

3. Results and discussion

3.1. Structural characterization

The XRD of pure ZnO nanoparticles, PU/CS blend, and PU/CS/ZnO nanocomposite films with varying ZnO concentrations are presented in Figure 1. The XRD pattern of ZnO nanoparticles exhibited characteristic peaks at 2θ values of 31.7°, 34.4°, 36.2°, 47.5°, 56.6°, 62.8° , corresponding to the (100), (002), (101), (102), (110), and planes [20], respectively. The distinct and strong peaks suggest that the ZnO nanoparticles synthesized have a high level of crystallinity [21].

The XRD pattern of the PU/CS blend showed a broad peak centered at 2θ = 20.5°, characteristic of the amorphous nature of the polymer blend. Upon incorporation of ZnO nanoparticles, the nanocomposite films exhibited peaks corresponding to both the polymer blend and ZnO [22]. The intensity of ZnO peaks increased with increasing nanoparticle concentration, confirming the successful incorporation of ZnO into the polymer matrix [23]. The average size of ZnO nanoparticles was determined to be 28 ± 2 nm, indicating the presence of small crystallites.

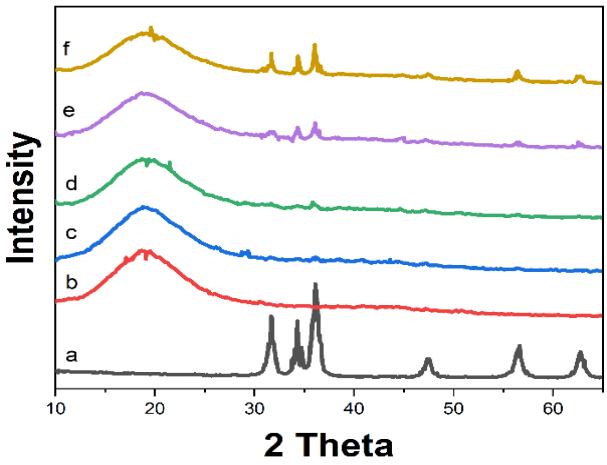

Fig. 1. XRD patterns of (a) ZnO nanoparticles, (b) PU/CS blend, (c) PU/CS/ZnO-1%, (d) PU/CS/ZnO-3%, (e) PU/CS/ZnO-5%, and (f) PU/CS/ZnO-7% nanocomposite films.

3.2. FTIR spectroscopy

The FTIR spectra of pure PU, CS, ZnO nanoparticles, and the PU/CS/ZnO nanocomposite films are illustrated in Figure 2. The PU FTIR spectrum displayed distinctive peaks at 3320 cm-1 for N-H stretching, 2940 cm^{-1} and 2860 cm^{-1} for symmetric and asymmetric CH_2 stretching, 1730 cm^{-1} for C=O stretching of urethane, and 1535 cm^{-1} for N-H bending and C-N stretching [24]. The CS spectrum showed peaks at 3450 cm^{-1} (O-H stretching), 2880 cm^{-1} (C-H stretching), 1655 cm^{-1} (amide I), and 1590 cm^{-1} (N-H bending of amino group).

The FTIR spectrum of ZnO nanoparticles displayed a strong absorption band at 435 cm^{-1}. In the PU/CS/ZnO nanocomposite films, the characteristic peaks of both PU and CS were observed, indicating the successful blending of the two polymers. The intensity of the Zn-O peak at 435 cm^{-1} increased with increasing ZnO concentration in the nanocomposites [25]. Interestingly, a slight shift in the N-H stretching peak of PU from 3320 cm^{-1} to 3340 cm^{-1} was observed in the nanocomposite films. This change indicates that hydrogen bonds may be forming between the N-H groups of PU and the hydroxyl groups on the ZnO nanoparticles' surface, demonstrating strong interfacial interaction between the nanoparticles and the polymer matrix [26].

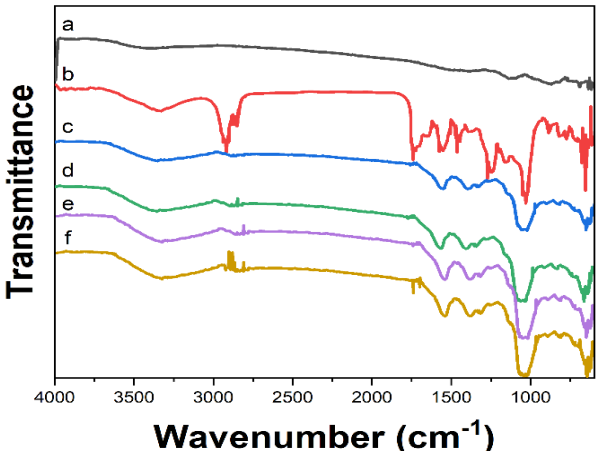

Fig. 2. FTIR spectra of (a) pure PU, (b) pure CS, (c) ZnO nanoparticles, (d) PU/CS blend, (e) PU/CS/ZnO-3%, and (f) PU/CS/ZnO-5% nanocomposite films.

3.3. Morphology and dispersion of ZnO nanoparticles

The morphology and dispersion of ZnO nanoparticles within the PU/CS matrix were investigated using SEM and TEM techniques. Figure 3 presents the SEM of the surface and cross-section of PU/CS blend and PU/CS/ZnO nanocomposite films with 5 wt% ZnO loading. The PU/CS blend exhibited a smooth and homogeneous surface, indicating good compatibility between the two polymers [27]. In contrast, the nanocomposite film showed a rougher surface with visible ZnO nanoparticles distributed across the polymer matrix.

The SEM images showed a distinct layered arrangement in the PU/CS blend, which is believed to be a result of the separation of the two polymers into distinct phases. The incorporation of ZnO nanoparticles appeared to disrupt this layered structure, resulting in a more homogeneous cross-section. This finding indicates that the presence of ZnO nanoparticles could potentially enhance the blending of PU and CS by acting as a compatibilizer.

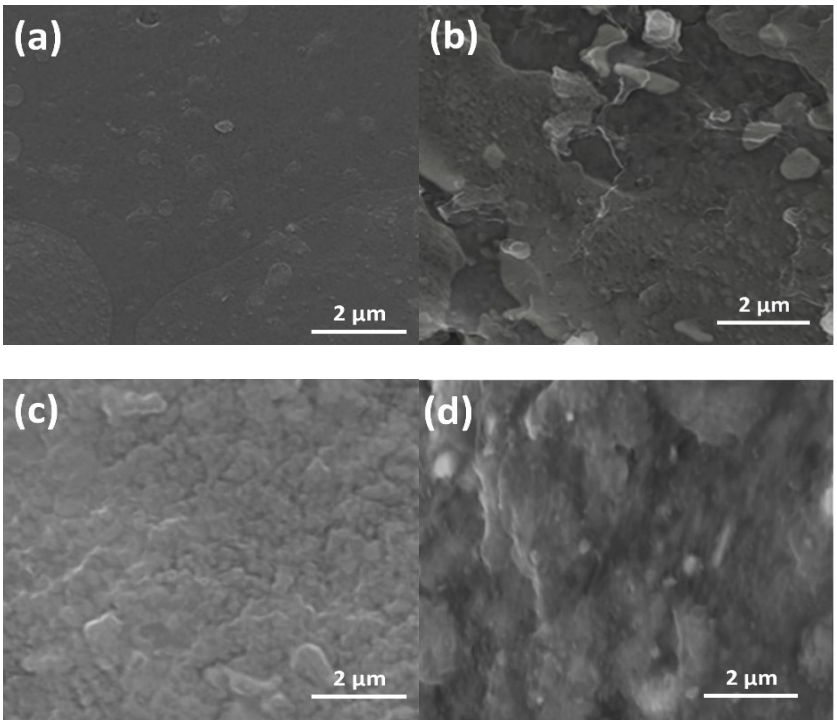

Fig. 3. SEM of (a) surface and (b) cross-section of PU/CS blend; (c) surface and (d) cross-section of PU/CS/ZnO-5% nanocomposite film.

3.4. Mechanical properties

The mechanical properties of PU/CS blend and PU/CS/ZnO nanocomposite films were evaluated through tensile testing. Figure 4 presents the stress-strain curves for the samples, while Table 1 summarizes the key mechanical parameters including tensile strength, Young's modulus, and elongation at break.

The incorporation of ZnO nanoparticles led to a significant enhancement in the tensile strength of the nanocomposite films. The pure PU/CS blend exhibited a tensile strength of 18.2 ± 0.8 MPa. With the addition of ZnO nanoparticles, the tensile strength increased progressively,

reaching a maximum of 27.5 ± 1.2 MPa for the PU/CS/ZnO-5% nanocomposite, representing a 51% improvement. This enhancement can be attributed to the reinforcing effect of ZnO nanoparticles and their good interfacial interaction with the polymer matrix, as evidenced by the FTIR analysis.

However, a slight decrease in tensile strength was observed for the PU/CS/ZnO-7% sample (25.8 ± 1.5 MPa). This reduction is likely due to the agglomeration of nanoparticles at higher concentrations, as observed in the TEM analysis, which can create stress concentration points and weaken the overall structure.

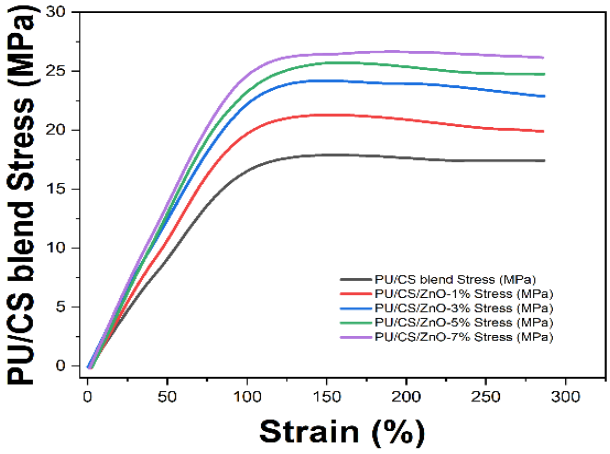

Fig. 4. Stress-strain curves of PU/CS blend and PU/CS/ZnO nanocomposite films with varying ZnO concentrations.

Table 1. Mechanical properties of PU/CS blend and PU/CS/ZnO nanocomposite films.

Sample	**Tensile Strength (MPa)**	**Young's Modulus (MPa)**	**Elongation at Break (%)**
PU/CS blend	18.2 ± 0.8	245 ± 12	285 ± 15
PU/CS/ZnO-1%	21.7 ± 1.0	298 ± 15	248 ± 13
PU/CS/ZnO-3%	24.9 ± 1.1	356 ± 17	215 ± 11
PU/CS/ZnO-5%	27.5 ± 1.2	412 ± 18	180 ± 10
PU/CS/ZnO-7%	25.8 ± 1.5	395 ± 20	162 ± 12

The Young's modulus, indicative of the material's stiffness, showed a similar trend to tensile strength. The PU/CS blend had a Young's modulus of 245 ± 12 MPa, which increased with ZnO nanoparticle incorporation. The PU/CS/ZnO-5% nanocomposite exhibited the highest Young's modulus of 412 ± 18 MPa, representing a 68% increase compared to the pure blend. This significant improvement in stiffness can be attributed to the high modulus of ZnO nanoparticles and their ability to restrict the mobility of polymer chains [28]. The PU/CS/ZnO-7% sample showed a slight decrease in Young's modulus (395 ± 20 MPa) compared to the 5% loading, further supporting the notion that nanoparticle agglomeration at higher concentrations can compromise the mechanical properties.

The elongation at break, a measure of the material's ductility, showed an inverse relationship with ZnO nanoparticle concentration. The pure PU/CS blend exhibited an elongation at break of 285 ± 15%. As ZnO nanoparticles were incorporated, the elongation at break decreased progressively, reaching 180 ± 10% for the PU/CS/ZnO-5% nanocomposite. This reduction in ductility is a common observation in nanocomposite systems and can be attributed to the restricting effect of nanoparticles on polymer chain mobility [29]. Despite the decrease, the nanocomposite films retained considerable flexibility, which is crucial for packaging applications.

3.5. Barrier properties

The films were evaluated for their ability to block water vapor by determining their water vapor transmission rate (WVTR). Figure 5 illustrates the WVTR values for the PU/CS blend and PU/CS/ZnO nanocomposite films. The pure PU/CS blend exhibited a WVTR of 24.5 ± 1.2 g/m^2/day. The addition of ZnO led to a reduction in WVTR, with the PU/CS/ZnO-5% nanocomposite showing the lowest value of 12.8 ± 0.7 g/m^2/day, representing a 48% improvement in water vapor barrier properties.

This enhancement can be attributed to two factors: 1) The impermeable nature of ZnO nanoparticles, which create a tortuous path for water vapor molecules, increasing their diffusion path length. 2) The effective bonding between ZnO nanoparticles and the polymer matrix limits the space for water vapor to pass through [30]. Interestingly, the PU/CS/ZnO-7% sample showed a slight increase in WVTR (13.5 ± 0.8 g/m^2/day) compared to the 5% loading. This could be due to the nanoparticle agglomeration observed at higher concentrations, which may create micro-voids in the polymer matrix, facilitating water vapor transmission [31].

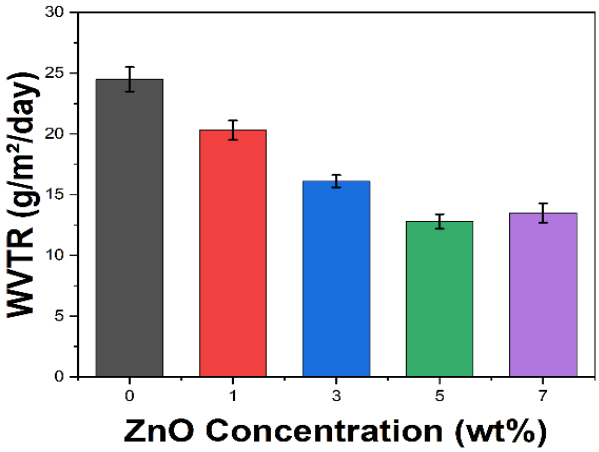

Fig. 5. WVTR of PU/CS blend and PU/CS/ZnO nanocomposite films as a function of ZnO nanoparticle concentration.

The films were assessed for their ability to block oxygen by analyzing their oxygen permeability. Table 2 presents the oxygen permeability values for the PU/CS blend and PU/CS/ZnO nanocomposite films. The pure PU/CS blend showed an oxygen permeability of 18.2 ± 0.9 cm^3.µm/m^2.day.kPa. The addition of ZnO nanoparticles resulted in a significant decrease in the

permeability of oxygen. The PU/CS/ZnO-5% nanocomposite exhibited the lowest oxygen permeability of 7.5 ± 0.4 cm^3.μm/m^2.day.kPa, representing a 59% improvement in oxygen barrier properties.

This significant enhancement in oxygen barrier properties can be attributed to the same factors influencing water vapor transmission: the tortuous path created by impermeable ZnO nanoparticles and the reduction in free volume due to strong interfacial interactions [32]. Similar to the trend observed in WVTR, the PU/CS/ZnO-7% sample showed a slight increase in oxygen permeability (8.1 ± 0.5 cm^3.μm/m^2.day.kPa) compared to the 5% loading, further supporting the notion that excessive nanoparticle loading can compromise the barrier properties due to agglomeration.

The improved barrier properties of the PU/CS/ZnO nanocomposite films against both water vapor and oxygen make them promising candidates for food packaging applications, where maintaining product freshness and preventing oxidation are crucial.

Table 2. Oxygen permeability of PU/CS blend and PU/CS/ZnO nanocomposite films.

Sample	**Oxygen Permeability (cm^3·μm/m^2·day·kPa)**
PU/CS blend	18.2 ± 0.9
PU/CS/ZnO-1%	14.7 ± 0.7
PU/CS/ZnO-3%	10.3 ± 0.5
PU/CS/ZnO-5%	7.5 ± 0.4
PU/CS/ZnO-7%	8.1 ± 0.5

3.6. Optical properties

The optical properties of the PU/CS blend and PU/CS/ZnO nanocomposite films were investigated using UV-visible spectroscopy. Figure 6 displays the UV-vis transmittance spectra of the films, spanning from 200 to 800 nm. The pure blend of PU/CS showed excellent transparency in the visible spectrum (400-800 nm) with an average transmittance of 89%. This high transparency is advantageous for packaging applications where visual inspection of the contents is desired [33]. Upon incorporation of ZnO nanoparticles, a gradual decrease in transmittance was observed across the entire spectrum.

The PU/CS/ZnO-1% nanocomposite maintained relatively high transparency with an average visible light transmittance of 82%. As the ZnO concentration increased, the transmittance decreased further, with the PU/CS/ZnO-5% and PU/CS/ZnO-7% samples showing average visible light transmittances of 68% and 61%, respectively. This reduction in transparency can be attributed to the scattering of light by ZnO nanoparticles dispersed within the polymer matrix [34]. Interestingly, all nanocomposite films exhibited a sharp decrease in transmittance at wavelengths below 380 nm, corresponding to the UV region. This behavior is indicative of the UV-blocking ability of the nanocomposite films, which is further explored in the following section.

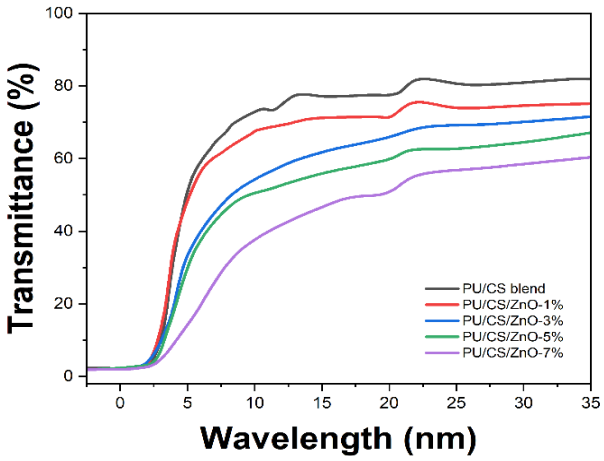

Fig. 6. UV-vis transmittance spectra of PU/CS blend and PU/CS/ZnO nanocomposite films with varying ZnO concentrations.

The UV blocking ability of the films was quantified by calculating the UV protection factor (UPF) based on the transmittance data. The UPF values for the PU/CS blend and PU/CS/ZnO nanocomposite films are presented in Table 3. The pure PU/CS blend showed minimal UV protection with a UPF value of 1.8. However, the incorporation of ZnO nanoparticles led to a dramatic increase in UV protection [35]. The PU/CS/ZnO-1% nanocomposite exhibited a UPF of 15.3, which is classified as good UV protection. As the ZnO concentration increased, the UPF values improved significantly, with the PU/CS/ZnO-5% and PU/CS/ZnO-7% samples achieving UPF values of 42.7 and 51.2, respectively, both classified as excellent UV protection.

The exceptional UV blocking ability of the nanocomposite films can be attributed to the intrinsic UV absorption properties of ZnO nanoparticles. ZnO has a wide bandgap (3.37 eV) that allows it to absorb UV radiation effectively. This property, combined with the uniform dispersion of ZnO nanoparticles throughout the polymer matrix, results in efficient UV blocking across the film.

The enhanced UV protection offered by the PU/CS/ZnO nanocomposite films is particularly beneficial for packaging applications where UV-induced degradation of contents needs to be prevented, such as in food packaging or for UV-sensitive products.

Table 3. UPF values for PU/CS blend and PU/CS/ZnO nanocomposite films.

Sample	**UV Protection Factor (UPF)**	**Protection Category**
PU/CS blend	1.8 ± 0.2	No protection
PU/CS/ZnO-1%	15.3 ± 0.8	Good
PU/CS/ZnO-3%	28.6 ± 1.4	Very Good
PU/CS/ZnO-5%	42.7 ± 1.6	Excellent
PU/CS/ZnO-7%	51.2 ± 2.5	Excellent

3.6. Antioxidant properties

The antioxidant activity of the PU/CS blend and PU/CS/ZnO nanocomposite films was evaluated using the DPPH radical scavenging assay. This method assesses the ability of the films to neutralize free radicals, which is crucial for preventing oxidative degradation of packaged food products. Figure 7 presents the DPPH radical scavenging activity of the films as a function of ZnO nanoparticle concentration. The pure PU/CS blend exhibited a moderate antioxidant activity with a DPPH radical scavenging percentage of 32.5 ± 2.1%. This baseline activity can be attributed to the presence of amino groups in CS, which can donate electrons to neutralize free radicals [36]. Upon incorporation of ZnO nanoparticles, a significant enhancement in antioxidant activity was observed.

The PU/CS/ZnO-1% nanocomposite showed a DPPH radical scavenging activity of 45.7 ± 2.8%, representing a 40.6% increase compared to the pure blend. As the ZnO concentration increased, the antioxidant activity improved further, reaching a maximum of 68.3 ± 3.2% for the PU/CS/ZnO-5% nanocomposite. This corresponds to a remarkable 110% enhancement in antioxidant activity compared to the pure PU/CS blend. Interestingly, the PU/CS/ZnO-7% sample showed a slight decrease in antioxidant activity (65.9 ± 3.5%) compared to the 5% loading. This minor reduction could be attributed to the agglomeration of ZnO nanoparticles at higher concentrations, which may reduce the effective surface area available for radical scavenging [37].

The enhanced antioxidant activity of the nanocomposite films can be explained by several factors:

1. Synergistic effect: The combination of CS's inherent antioxidant properties and the radical scavenging ability of ZnO nanoparticles creates a synergistic effect.

2. Surface reactivity: The high surface-to-volume ratio of ZnO nanoparticles provides numerous active sites for radical neutralization.

3. Electron donation: ZnO nanoparticles can donate electrons to neutralize free radicals, complementing the electron-donating capacity of CS.

The improved antioxidant properties of the PU/CS/ZnO nanocomposite films make them particularly suitable for packaging applications where preventing oxidative degradation of contents is crucial, such as in the preservation of lipid-rich foods or oxygen-sensitive products [38].

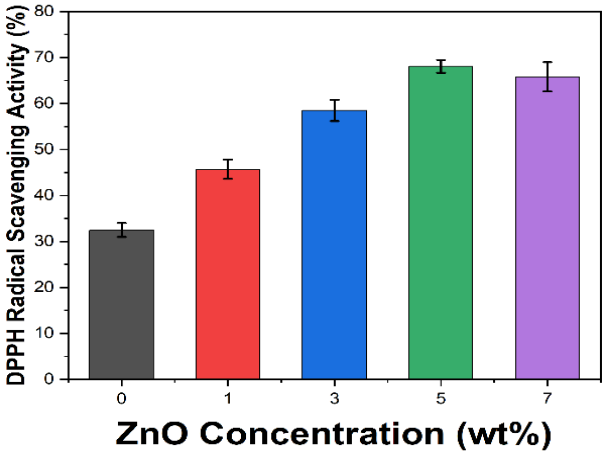

Fig. 7. DPPH radical scavenging activity of PU/CS blend and PU/CS/ZnO nanocomposite films as a function of ZnO nanoparticle concentration.

3.7. Biodegradability

The degradation of the PU/CS blend and PU/CS/ZnO nanocomposite films was evaluated by burying them in soil for a duration of 12 weeks. Figure 8 illustrates the weight loss percentage of the films as a function of burial time, while Table 4 summarizes the final weight loss and degradation rate constants. The pure PU/CS blend demonstrated significant biodegradability, with a weight loss of 72.3 ± 3.5% after 12 weeks of soil burial. This high degradation rate can be attributed to the presence of biodegradable CS in the blend, which can be readily broken down by soil microorganisms. Incorporation of ZnO nanoparticles led to a moderate reduction in the biodegradation rate. The PU/CS/ZnO-1% nanocomposite exhibited a weight loss of 65.8 ± 3.2% after 12 weeks, while the PU/CS/ZnO-5% sample showed a weight loss of 58.1 ± 2.9%. This trend of decreasing biodegradability with increasing ZnO concentration can be explained by several factors:

1. Antimicrobial activity: The antibacterial properties of ZnO nanoparticles may inhibit the growth and activity of soil microorganisms responsible for biodegradation.

2. Physical barrier: Well-dispersed ZnO nanoparticles can create a physical barrier, reducing the accessibility of polymer chains to degrading enzymes.

3. Crosslinking effect: The strong interactions between ZnO nanoparticles and the polymer matrix may create a crosslinking effect, slowing down the degradation process.

The degradation rate constant decreased from 0.108 $week^{-1}$ for the pure PU/CS blend to 0.073 $week^{-1}$ for the PU/CS/ZnO-5% nanocomposite. Despite the reduction in degradation rate, all nanocomposite films maintained substantial biodegradability, with more than 50% weight loss after 12 weeks.

The biodegradability results demonstrate that while the incorporation of ZnO nanoparticles moderately slows down the degradation process, the PU/CS/ZnO nanocomposite films still retain significant biodegradability. This characteristic is crucial for developing environmentally friendly packaging materials that can decompose naturally after disposal, thereby reducing environmental impact.

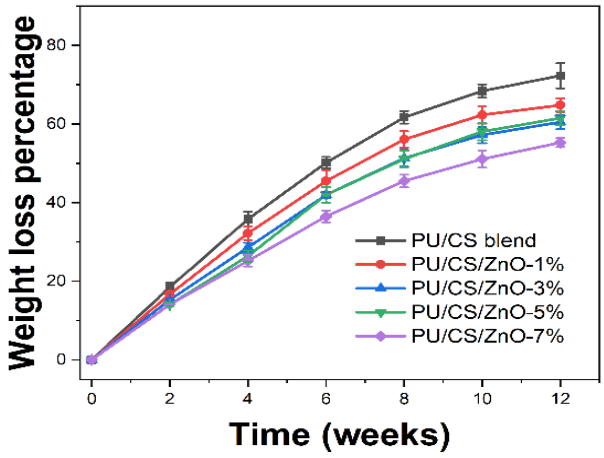

Fig. 8. Weight loss percentage of PU/CS blend and PU/CS/ZnO nanocomposite films during soil burial test over 12 weeks.

Table 4. Final weight loss percentages and degradation rate constants (k) for PU/CS blend and PU/CS/ZnO nanocomposite films after 12 weeks of soil burial.

Sample	Final Weight Loss (%)	Degradation Rate Constant k ($week^{-1}$)
PU/CS blend	72.3	0.108
PU/CS/ZnO-1%	65.8	0.092
PU/CS/ZnO-3%	61.5	0.083
PU/CS/ZnO-5%	58.1	0.073
PU/CS/ZnO-7%	55.7	0.068

3.8. Application in food packaging

To evaluate the practical efficacy of the developed PU/CS/ZnO nanocomposite films in food packaging applications, shelf-life extension studies were conducted using fresh strawberries as a model perishable food product. The strawberries were packaged in the PU/CS blend and PU/CS/ZnO-5% nanocomposite films, with commercially available low-density polyethylene (LDPE) film used as a control. The strawberries in their packaging were kept in a refrigerator at a temperature of 4°C for a period of 14 days, during which time a range of quality indicators were regularly assessed.

Figure 9 presents the changes in weight loss, firmness, and total soluble solids (TSS) content of the strawberries over the storage period. Table 5 summarizes the microbial counts and overall acceptability scores at the end of the storage period. Weight loss: Strawberries packaged in the PU/CS/ZnO-5% nanocomposite film exhibited the lowest weight loss (4.2 ± 0.3%) after 14 days of storage, compared to those packaged in the PU/CS blend (6.8 ± 0.5%) and LDPE film (8.1 ± 0.6%). The decreased amount of weight loss can be credited to the enhanced water vapor barrier characteristics of the nanocomposite film, aiding in the preservation of the strawberries' moisture levels.

Firmness: The firmness of strawberries, measured using a texture analyzer, showed a similar trend. Strawberries packaged in the PU/CS/ZnO-5% nanocomposite film retained 78.5 ± 2.1% of their initial firmness after 14 days, compared to 65.3 ± 2.5% for the PU/CS blend and 58.7 ± 2.8% for the LDPE film. The improved firmness retention can be attributed to the reduced moisture loss and the potential inhibition of cell wall-degrading enzymes due to the antioxidant properties of the nanocomposite film.

TSS: The TSS content, an indicator of sugar concentration and ripening, increased more slowly in strawberries packaged in the PU/CS/ZnO-5% nanocomposite film. After 14 days, the TSS content increased by 15.3 ± 0.8% for the nanocomposite film, compared to 22.7 ± 1.2% for the PU/CS blend and 28.5 ± 1.5% for the LDPE film. The slower increase in TSS content suggests delayed ripening and senescence, likely due to the reduced respiration rate facilitated by the improved oxygen barrier properties of the nanocomposite film.

Microbial growth: Table 5 shows that strawberries packaged in the PU/CS/ZnO-5% nanocomposite film had significantly lower microbial counts (total aerobic bacteria and yeast/mold) after 14 days of storage compared to those packaged in the PU/CS blend and LDPE film. This reduction in microbial growth can be attributed to the antimicrobial properties of the nanocomposite film, which helps prevent spoilage and maintain food safety.

Overall acceptability: Sensory evaluation conducted by a panel of trained judges revealed that strawberries packaged in the PU/CS/ZnO-5% nanocomposite film maintained the highest overall acceptability score after 14 days of storage. The improved retention of color, texture, and aroma contributed to the higher acceptability of these samples.

These results demonstrate that the PU/CS/ZnO nanocomposite film significantly extends the shelf life of strawberries compared to the pure PU/CS blend and conventional LDPE packaging. The enhanced performance can be attributed to the synergistic effects of improved barrier properties, antimicrobial activity, and antioxidant properties of the nanocomposite film. This study highlights the potential of PU/CS/ZnO nanocomposite films for use in active food packaging applications, particularly for highly perishable products like fresh fruits and vegetables.

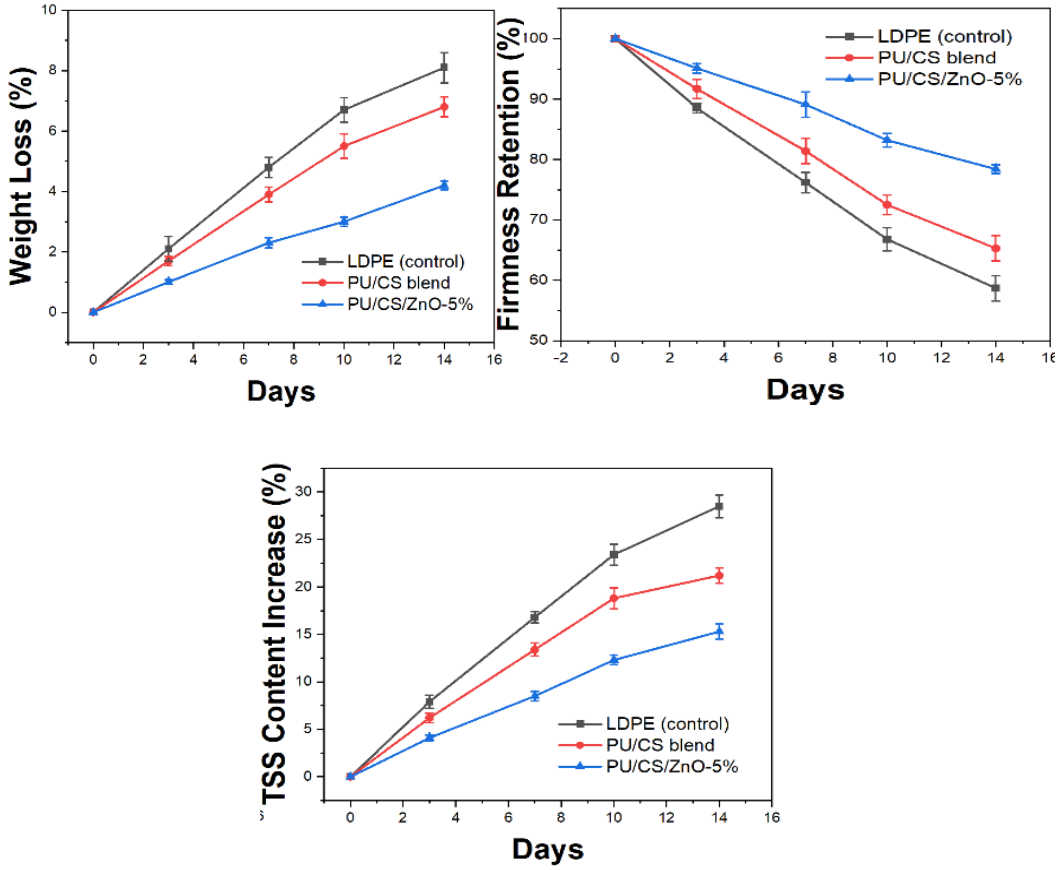

Fig. 9. Changes in (a) weight loss, (b) firmness, and (c) TSS content of strawberries packaged in different films during 14 days of storage at 4°C.

Table 5. Microbial counts (log CFU/g) and overall acceptability scores of strawberries packaged in different films after 14 days of storage at 4°C.

Packaging Film	**Total Aerobic Bacteria (log CFU/g)**	**Yeast and Mold (log CFU/g)**	**Overall Acceptability Score (1-9 scale)**
LDPE (control)	5.8 ± 0.3	4.7 ± 0.2	3.2 ± 0.4
PU/CS blend	4.9 ± 0.2	3.8 ± 0.2	5.1 ± 0.3
PU/CS/ZnO-5%	3.2 ± 0.2	2.5 ± 0.1	7.4 ± 0.3

4. Conclusion

This study successfully synthesized and characterized novel PU/CS/ZnO nanocomposite films for potential use in food packaging applications. The incorporation of ZnO nanoparticles, synthesized via a green approach using Mentha pulegium leaf extract, into the PU/CS blend resulted in significant improvements across multiple properties. The addition of 5% ZnO to the PU/CS blend resulted in significant enhancements in mechanical properties. Tensile strength increased by 51% to 27.5 MPa, while Young's modulus saw a 68% improvement to 412 MPa in the PU/CS/ZnO-5% nanocomposite. Barrier properties were substantially enhanced, with the PU/CS/ZnO-5% film showing a 48% reduction in water vapor transmission rate (12.8 g/m²/day) and a 59% decrease in oxygen permeability (7.5 cm³·μm/m²·day·kPa). The nanocomposite films demonstrated excellent UV protection, with the PU/CS/ZnO-5% sample achieving a UPF value of 42.7. Antioxidant activity was significantly improved, with the PU/CS/ZnO-5% film exhibiting a 110% increase in DPPH radical scavenging activity (68.3%) compared to the pure blend. While the incorporation of ZnO nanoparticles moderately reduced biodegradability, the PU/CS/ZnO-5% film still maintained substantial biodegradability with 58.1% weight loss after 12 weeks of soil burial. Shelf-life extension studies using strawberries demonstrated the practical efficacy of the nanocomposite films, with the PU/CS/ZnO-5% film significantly outperforming both the PU/CS blend and commercial LDPE film in terms of weight loss reduction, firmness retention, and microbial growth inhibition. After 14 days of storage, strawberries packaged in the PU/CS/ZnO-5% film showed the lowest weight loss (4.2%), highest firmness retention (78.5%), and lowest microbial counts (3.2 log CFU/g for total aerobic bacteria). These results highlight the potential of PU/CS/ZnO nanocomposite films as multifunctional, biodegradable packaging materials for extending the shelf life of perishable foods.

Acknowledgements

This work was supported by Key project of science and technology research program of Chongqing Education Commission of China (No. KJZD-K202403601) and Youth project of science and technology research program of Chongqing Education Commission of China (No. KJQN202303605).

References

[1] F. S. Mostafavi, D. Zaeim, International Journal of Biological Macromolecules 159, 1165 (2020); https://doi.org/10.1016/j.ijbiomac.2020.05.123

[2] C. L. Reichert, E. Bugnicourt, M.-B. Coltelli, P. Cinelli, A. Lazzeri, I. Canesi, F. Braca, B. M. Martínez, R. Alonso, L. Agostinis, S. Verstichel, L. Six, S. D. Mets, E. C. Gómez, C. Ißbrücker, R. Geerinck, D. F. Nettleton, I. Campos, E. Sauter, P. Pieczyk, M. Schmid, Polymers 12, 1558 (2020); https://doi.org/10.3390/polym12071558

[3] J. S. Yaradoddi, N. R. Banapurmath, S. V. Ganachari, M. E. M. Soudagar, N. M. Mubarak, S. Hallad, S. Hugar, H. Fayaz, Scientific Reports 10, 21960 (2020); https://doi.org/10.1038/s41598-

020-78912-z

[4] L. Zhao, G. Duan, G. Zhang, H. Yang, S. He, S. Jiang, Nanomaterials 10, 150 (2020); https://doi.org/10.3390/nano10010150

[5] A. Piotrowska-Kirschling, J. Brzeska, Polymers 12, 1205 (2020); https://doi.org/10.3390/polym12051205

[6] A. A. Maamoun,A. A. Mahmoud, Cellulose 29, 6323 (2022); https://doi.org/10.1007/s10570-022-04655-x

[7] Y. Cheng, Y. Wei, C. Fang, H. Li, J. Chen, J. Zhang, Z. Huang, Journal of Materials Research and Technology 15, 5316 (2021); https://doi.org/10.1016/j.jmrt.2021.10.126

[8] J. Xu, C.-Y. Fu, Y.-L. Tsai, C.-W. Wong, S. Hsu, Polymers 13, 326 (2021); https://doi.org/10.3390/polym13030326

[9] Z. Liu, Z. Qin, H. Jia, J. Xu, M. Liu, Z. Hou, Food Packaging and Shelf Life 37, 101064 (2023); https://doi.org/10.1016/j.fpsl.2023.101064

[10] J. Siddiqui, M. Taheri, A. U. Alam, M. J. Deen, (n.d.).

[11] C. S. Reig, A. D. Lopez, M. H. Ramos, V. A. C. Ballester, (n.d.).

[12] N. Bumbudsanpharoke, J. Choi, S. Ko, Journal of Nanoscience and Nanotechnology 15, 6357 (2015); https://doi.org/10.1166/jnn.2015.10847

[13] M. Abbas, M. Buntinx, W. Deferme, R. Peeters, Nanomaterials 9, 1494 (2019); https://doi.org/10.3390/nano9101494

[14] M. Zare, K. Namratha, S. Ilyas, A. Sultana, A. Hezam, S. L, M. A. Surmeneva, R. A. Surmenev, M. B. Nayan, S. Ramakrishna, S. Mathur, K. Byrappa, ACS Food Science & Technology (2022).

[15] H. Zhang, M. Hortal, M. Jordá-Beneyto, E. Rosa, M. Lara-Lledo, I. Lorente, LWT 78, 250 (2017); https://doi.org/10.1016/j.lwt.2016.12.024

[16] J. Seo, G. Jeon, Eu. S. Jang, S. B. Khan, H. Han, (n.d.).

[17] E. Lizundia, L. Ruiz-Rubio, J. L. Vilas, L. M. León, (n.d.).

[18] H. M. Alghamdi, M. M. Abutalib, M. A. Mannaa, O. Nur, E. M. Abdelrazek, A. Rajeh, Journal of Materials Research and Technology 19, 3421 (2022); https://doi.org/10.1016/j.jmrt.2022.06.077

[19] R. Verma, S. Pathak, A. K. Srivastava, S. Prawer, S. Tomljenovic-Hanic, Journal of Alloys and Compounds 876, 160175 (2021); https://doi.org/10.1016/j.jallcom.2021.160175

[20] V. N. Kalpana, V. D. Rajeswari, (n.d.).

[21] R. A. Gonçalves, R. P. Toledo, N. Joshi, O. M. Berengue, Molecules 26, 2236 (2021); https://doi.org/10.3390/molecules26082236

[22] A. M. El Saeed, M. A. El-Fattah, A. M. Azzam, Dyes and Pigments 121, 282 (2015); https://doi.org/10.1016/j.dyepig.2015.05.037

[23] S. Kumar, M. M. Rahman, S. Yoon, S. Kim, N. Oh, K. H. Hong, J. Koh, Fibers and Polymers 22, 2227 (2021); https://doi.org/10.1007/s12221-021-0815-2

[24] D. Kim, K. Jeon, Y. Lee, J. Seo, K. Seo, H. Han, S. Khan, Progress in Organic Coatings 74, 435 (2012); https://doi.org/10.1016/j.porgcoat.2012.01.007

[25] R. R. Soares, C. Carone, S. Einloft, R. Ligabue, W. F. Monteiro, Polymer Bulletin 71, 829

(2014); https://doi.org/10.1007/s00289-014-1095-4

[26] A. Anand, R. D. Kulkarni, V. V. Gite, Coatings Science International 2011 74, 764 (2012); https://doi.org/10.1016/j.porgcoat.2011.09.031

[27] K. Rajitha, K. N. S. Mohana, M. B. Hegde, S. R. Nayak, N. K. Swamy, FlatChem 24, 100208 (2020); https://doi.org/10.1016/j.flatc.2020.100208

[28] J. Pavličević, M. Špírková, O. Bera, M. Jovičić, B. Pilić, S. Baloš, J. Budinski-Simendić, Composites Part B: Engineering 60, 673 (2014); https://doi.org/10.1016/j.compositesb.2014.01.016

[29] M. Zahra, H. Ullah, M. Javed, S. Iqbal, J. Ali, H. Alrbyawi, Samia, N. Alwadai, B. Ibrahim Basha, A. Waseem, S. Sarfraz, A. Amjad, N. S. Awwad, H. A. Ibrahium, H. H. Somaily, Inorganic Chemistry Communications 144, 109916 (2022); https://doi.org/10.1016/j.inoche.2022.109916

[30] B. Adak, M. Joshi, B. S. Butola, Composites Part B: Engineering 176, 107303 (2019); https://doi.org/10.1016/j.compositesb.2019.107303

[31] P. Tayebi, A. Asefnejad, H. A. Khonakdar, Polymer-Plastics Technology and Materials (2021).

[32] M. Kathalewar, A. Sabnis, G. Waghoo, Progress in Organic Coatings 76, 1215 (2013); https://doi.org/10.1016/j.porgcoat.2013.03.027

[33] S. Mallakpour, V. Behranvand, European Polymer Journal 84, 377 (2016); https://doi.org/10.1016/j.eurpolymj.2016.09.028

[34] B. Soltani, M. Asghari, Membranes 7, 43 (2017); https://doi.org/10.3390/membranes7030043

[35] S. Zhang, D. Zhang, H. Bai, W. Ming, ACS Applied Nano Materials 3, 59 (2020); https://doi.org/10.1021/acsanm.9b01540

[36] M. Amina, N. M. Al Musayeib, N. A. Alarfaj, M. F. El-Tohamy, G. A. Al-Hamoud, H. M. Al-yousef, Pharmaceutics 13, 2197 (2021); https://doi.org/10.3390/pharmaceutics13122197

[37] K. Marycz, M. Marędziak, J. Grzesiak, D. Szarek, A. Lis, J. Laska, Polymers 8, 175 (2016); https://doi.org/10.3390/polym8050175

[38] Y. Wang, H. Wang, Z. Li, D. Yang, X. Qiu, Y. Liu, M. Yan, Q. Li, Journal of Colloid and Interface Science 594, 316 (2021); https://doi.org/10.1016/j.jcis.2021.03.033